Quantifying complex changes resulting from recent climate warming to water bodies, surficial landforms, and vegetation in ice-wedge-polygon landscapes, Deadhorse, Alaska

Hannah Chapman-Dutton[1], Briana McNeal[2], Donald A. Walker[2]

Introduction

Arctic thaw-lake landscapes in northern Alaska are changing rapidly in response climate warming (e.g., Jorgenson et al. 2006, Raynolds et al. 2014, Liljedahl et al. 2016). The amount of change varies depending on the underlying surficial geology and the amount of ground ice in the surface deposits (Rawlinson 1993). This poster documents the changes that occurred between 1988 and 2020 to surficial landforms and vegetation in three areas representative of common surficial geology units of the **Natural Ice-Rich Permafrost Observatory (NIRPO,** Walker et al. 2024) , Prudhoe Bay Oilfield, Deadhorse, Alaska.

This area lies on the ecotone between the High and Low Arctic and is part of a unique regional biome associated with loess deposition from rivers flowing out of the limestone mountains of the Brooks Range (Walker et al. 1980. Walker 1985, Walker and Everett 1991). The area has flat, oriented-thaw-lake plain landscapes,, drained lake basins, the largest most diverse pingo field in North America, rich soils, marl-bottomed lakes, ice-wedge polygons, diverse calcareous tundra vegetation, and a rich assemblage of wildlife, including the calving grounds of the Central Arctic Caribou Herd, grizzly bears, Arctic ground squirrels, breeding grounds for many species of shorebirds and waterfowl, and large herds of muskoxen that feed on the diverse forage of the braided Sagavanirktok River floodplain.

Methods

Fig 1. The NIRPO site is situated near the Deadhorse Service Area of the Prudhoe Bay Oilfield. Four transects were surveyed in three typical thaw-lake landscapes.. Transects T6–T8 are 200-m long, and T9 is 100 m long. **T6, Residual surface,** is on an older ice-rich landscape that has not been subjected to thaw-lake processes (note: most of the thermokarst ponds on residual surfaces in this 2020 image were not present in 1988, see Fig . 2 detail of T6 imagery in 1988 and 2020) ; **T7, Ice-rich drained thaw lake basin**, is in an older drained thaw-lake basin with large well-developed ice-wedge polygons; and **T8, Ice-poor drained thaw lake basins,** is in a relatively young, recently drained thaw lake basin with mainly incipient, disjunct ice-wedge polygona. **Transect T9** is 100 m long and traverses portions of an ice-poor drained lake basin, three ancient shorelines, and a residual surface.

Fig 2. We used high-resolution aerial imagery to make photo-interpreted vegetation and landform maps of the areas surrounding the transect in 1988 (before recent rapid warming), and 2020 (after major transformation of ice-rich landscapes). **Legends** for the maps are below. **Fig. 3.** We used Sankey flow diagrams (Bostok, et al., 2011) to illustrate the changes to landforms and vegetation in each landscape and year. The diagram visually represent the change from the 1988 to the 2020 state, with the width of the connecting lines proportional to the quantity of flow.

Figure 1. Transect Locations

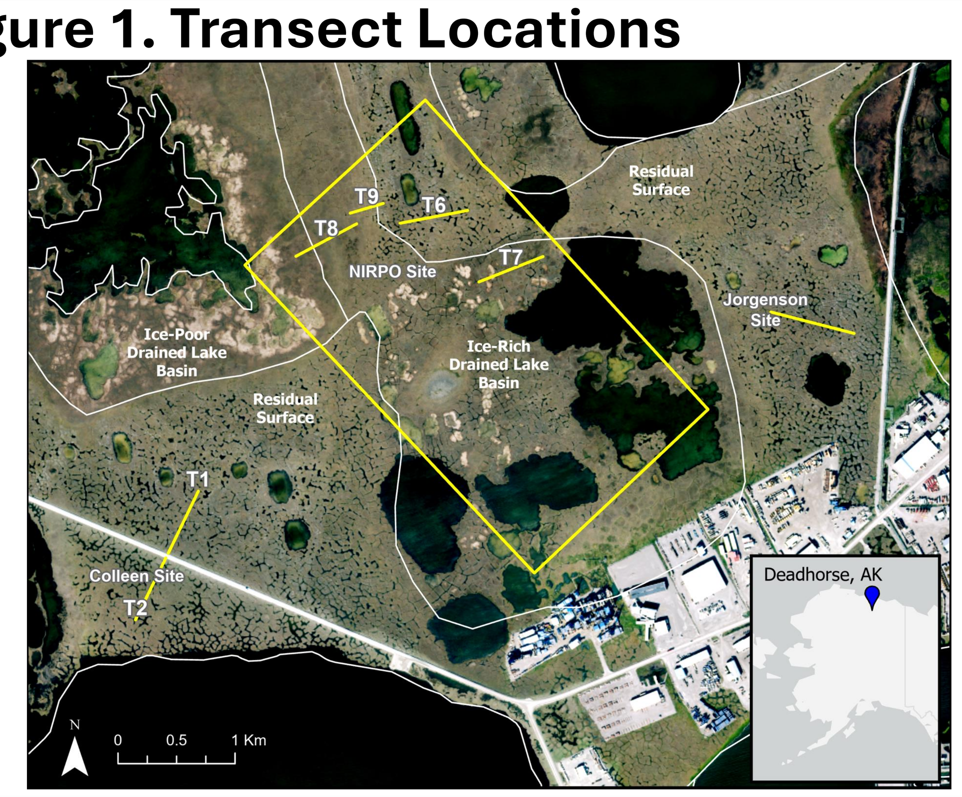

Map legends

Vegetation

- L1 — Lakes and deeper water generally >1m deep
- L2 — Shallow ponds with and lakes with marl bottoms
- L3 — Thermokarst ponds with sparse undifferentiated vegetation
- M1 — Moist nonacidic tundra with abundant lichens
- M3 — Moist nonacidic tundra with few lichens
- M3t — Transitional moist nonacidic tundra due to drainage changes
- Mz1 — Moist zoogenic vegetation on bird mounds and moist animal disturbances
- W1 — Wet nonacidic mires with saturated soils
- W1t — Transitional wet nonacidic mires, most closely resembling type W1
- W2 — Very wet nonacidic mires with shallow standing water
- A1 — Aquatic sedge marsh
- A1t — Transitional aquatic vegetation dominated by sedges
- Dfb — Dry to wet nonacidic sparsely-vegetated frost-boils

Landforms

- L1 — Deeper lakes and ponds (>1m)
- L2 — Shallow lakes with marl bottoms
- L3 — Thermokarst ponds
- DP — Disjunct polygons, low-center polygons with discontinuous rims
- LCP1 — Low-center polygon basin (<0.3m basin-trough relief)
- LCP2 — Low-center polygon basin (>0.3m basin-trough relief)
- TP1 — Transitional polygon center (<0.5m center-trough relief)
- TP2 — Transitional polygon center (>0.5m center-trough relief)
- HCP1 — High-center or flat-center polygon center(<0.5m center-trough relief)
- HCP2 — High-center or flat-center polygon center(>0.5m center-trough relief)

Landform elements

- Bird Mound
- Rims. Includes rims of disjunct polygons, intact low-center polygons, and transitional polygons with remnant rims
- Troughs
- Frost Boils
- Non-patterned (featureless)

Presented at the 27th Arctic Science Summit Week, Boulder, CO, USA, 20-28 March 2025

Author affiliations:
[1]Geographic Information Network of Alaska, Geophysical Institute, University of Alaska Fairbanks
[2]Alaska Geobotany Center, Institute of Arctic Biology, University of Alaska Fairbanks

Funding: U.S. National Science Foundation, Navigating the New Arctic, grant nr. 1928237

Figure 2. Change maps

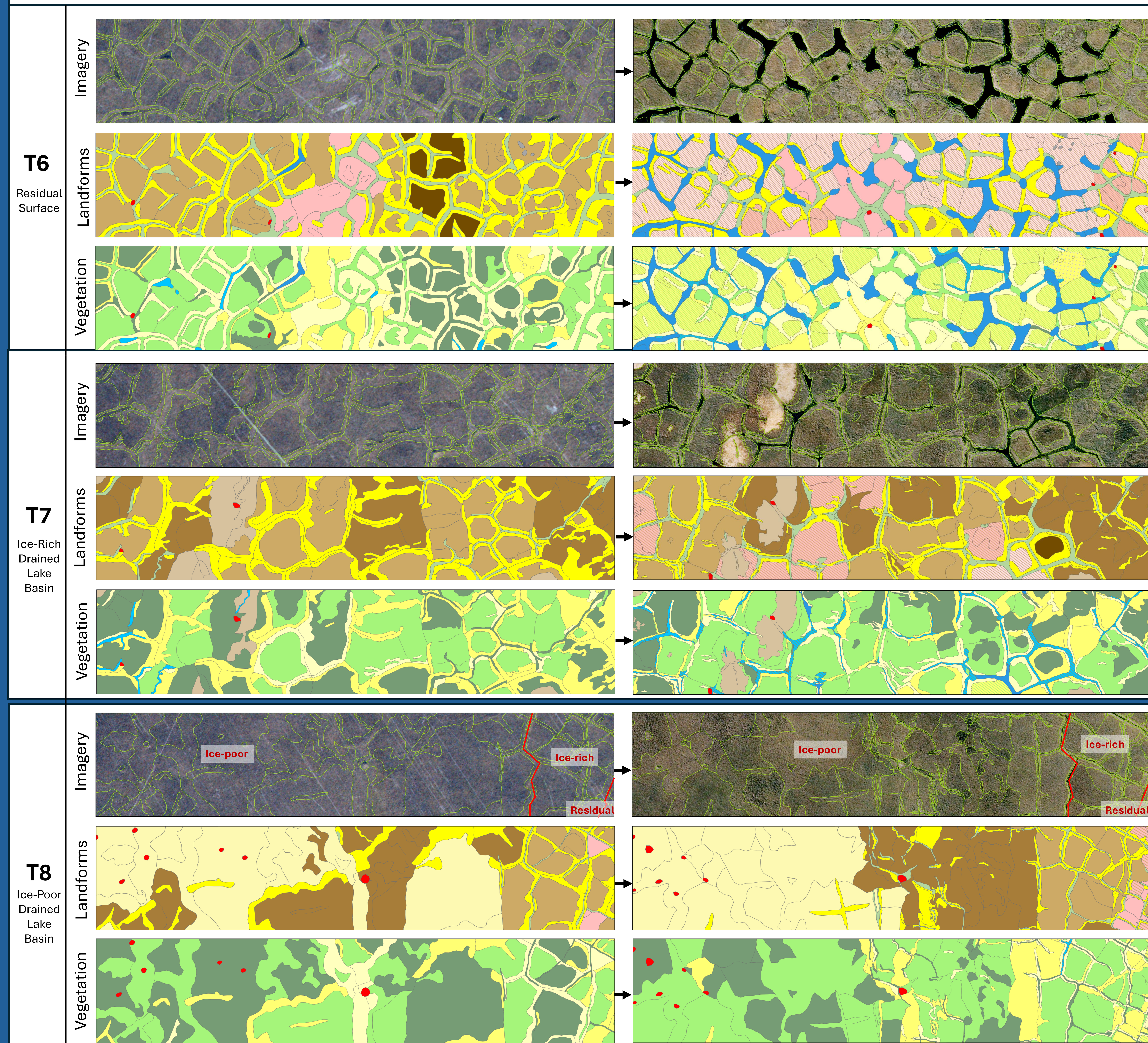

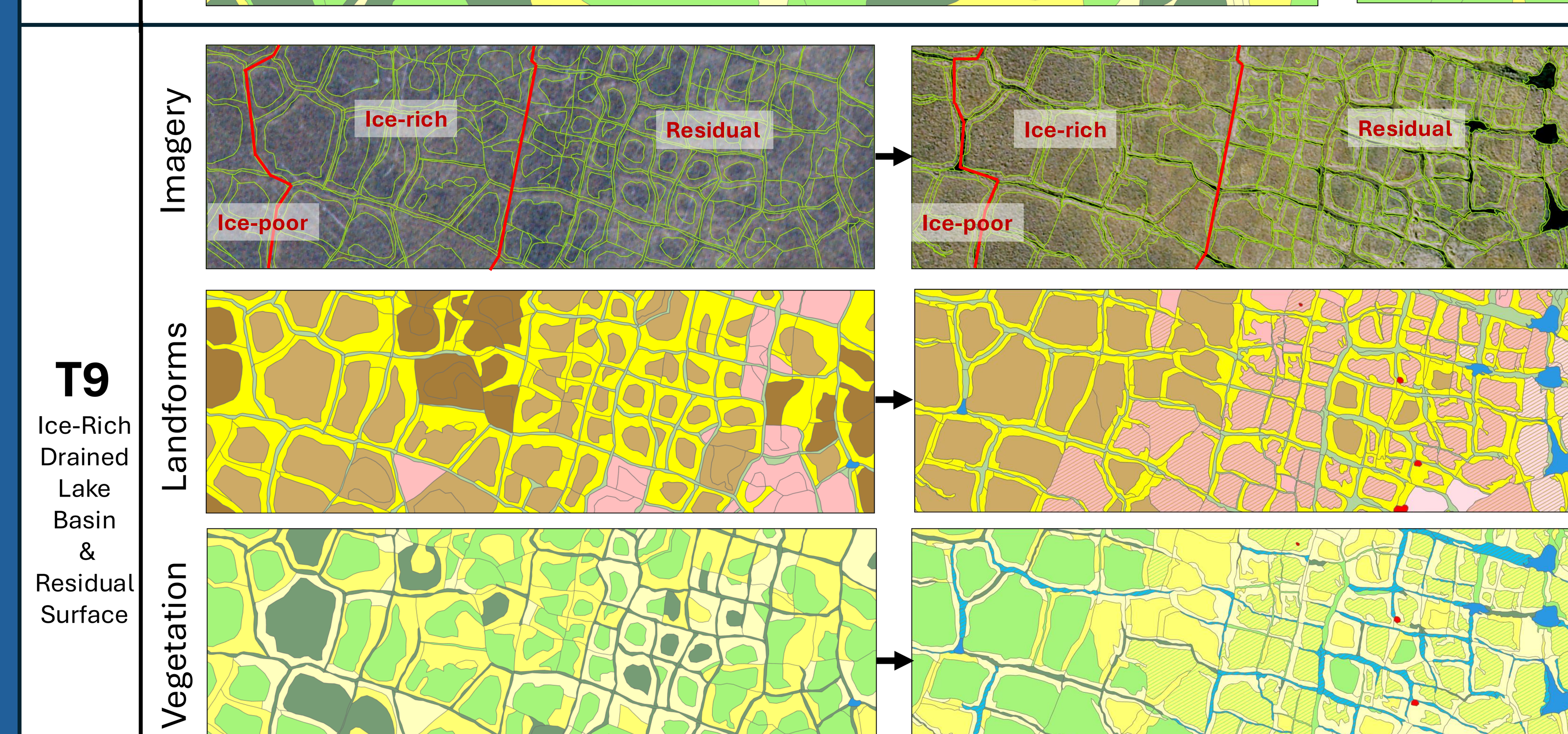

Conclusions

- The changes are related mostly to rapid development and expansion of thermokarst ponds, that began in the Prudhoe Bay region in the early 1990s (Raynolds et al. 2014, Walker et al. 2022).
- T6, the oldest landscape with large ice wedges, had the most change. Water in ponds and aquatic plant communities increased from less than 1% cover in 1988 to 13% in 2020. This was mainly a consequence of melting of the tops ice wedges, subsidence of the polygon troughs, accumulation of water in the troughs, and and drainage of the wet polygon basins into the troughs (Kanevesky et al. 2022).
- T7, the older drained lake basin had somewhat larger low-centered polygons with smaller ice-wedges than T6 in 1988 and showed less extensive changes to polygon morphology and vegetation.
- T8, the youngest surface in a recently drained lake basin, showed the least change because of fewer ice wedges.
- The resulting changes in water and nature of the vegetation dramatically effect ecosystem function (e.g. Kade et al. 2024).
- Detailed maps of patterned ground, such as these, are needed to help develop object-based pattern-recognition models of patterned-ground landscapes (e.g., Witharana et al. 2021).
- The maps provide a detailed picture of changes to water bodies, patterned-ground landforms, and vegetation in three different aged thaw-lake-plain landscapes with calcareous nonacidic vegetation. More attention needs to be directed at patterns of change in areas with different surficial geology and vegetation, such as in the sandy acidic tundra areas west of the Colville River, or the marine sediments of the Barrow area.

Figure 3a. Change analysis: *Landforms*

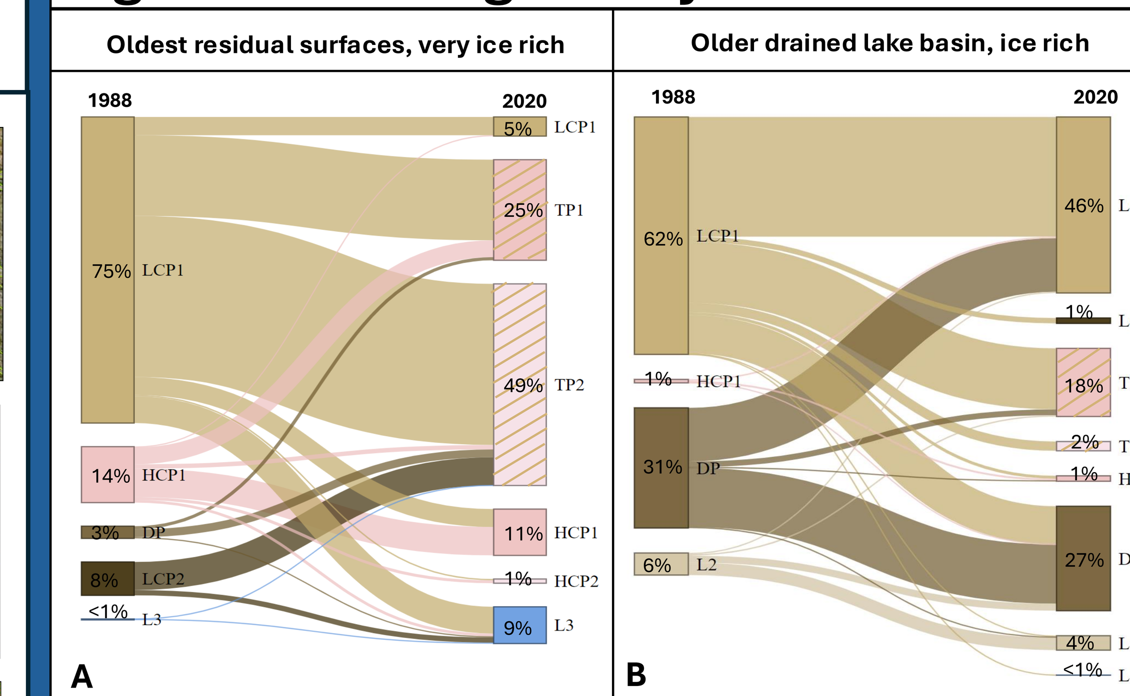

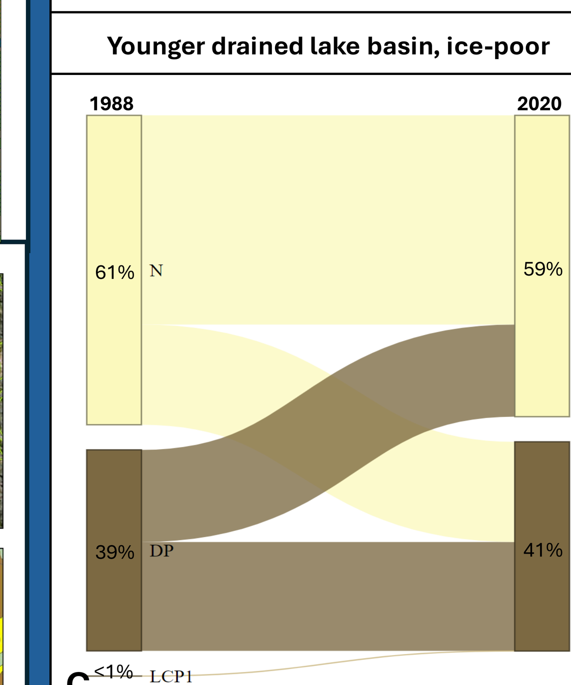

Summary of landform-change analysis results:

Surface	Landform	1988	2020
Residual surface	LCP1	74.9%	4.7%
	LCP2	8.1%	
	HCP1	13.7%	11.3%
	HCP2		1.0%
	TP1		24.6%
	TP2		49.4%
	DP	3.0%	
	L3	0.2%	9.0%
Ice-rich lake basin	LCP1	62.0%	46.0%
	LCP2		1.4%
	HCP1	0.9%	1.4%
	HCP2		
	TP1		17.8%
	TP2		2.4%
	DP	31.4%	27.3%
	L2	5.8%	3.8%
	L3		0.0%
Ice-poor lake basin	LCP1	0.03%	
	DP	39.4%	41.0%
	N	60.6%	59.0%

Figure 3b. Change analysis: *Vegetation*

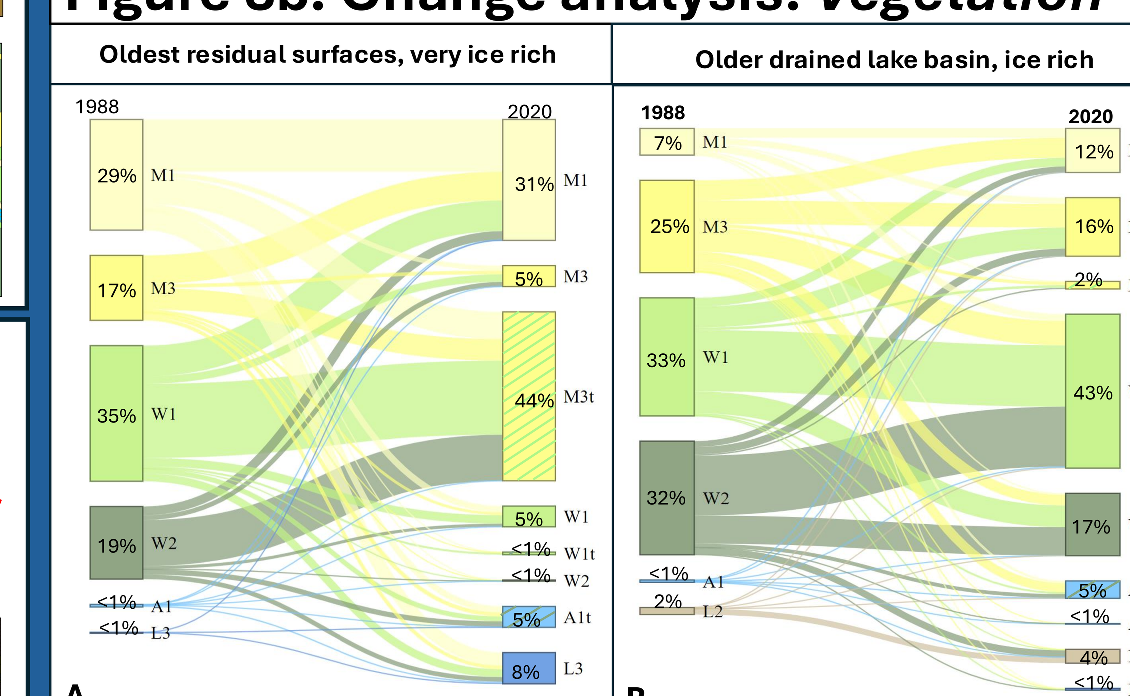

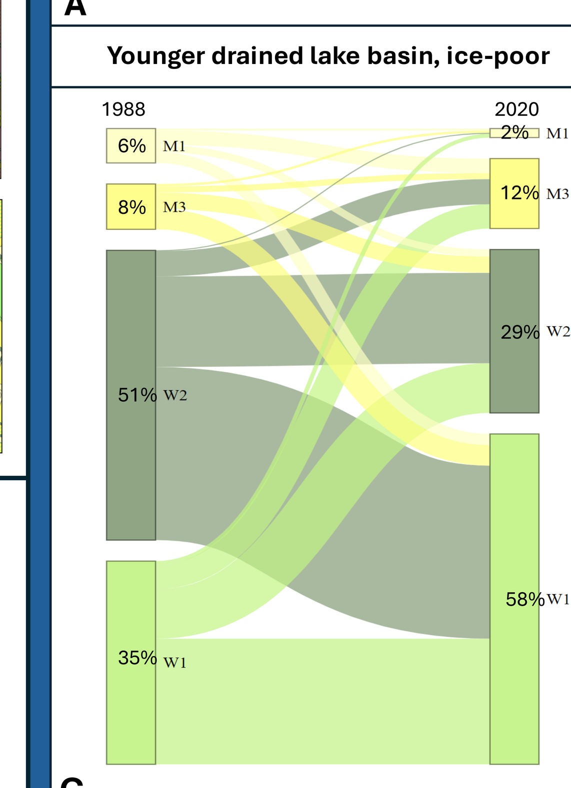

Summary of vegetation-change analysis results:

Surface	Vegetation	1988	2020
Residual surface	M1	28.6%	31.2%
	M3	16.8%	5.4%
	M3t		43.6%
	W1	35.0%	5.4%
	W1t		0.7%
	W2	18.8%	0.3%
	A1	0.7%	
	A1t		5.4%
	L3	0.2%	8.1%
Ice-rich lake basin	M1	7.4%	12.3%
	M3	25.6%	16.3%
	M3t		2.1%
	W1	32.8%	42.7%
	W2	31.6%	17.3%
	A1	0.7%	0.2%
	A1t		4.8%
	L2	2.0%	3.8%
	L3		0.5%
Ice-poor lake basin	M1	6.0%	1.6%
	M3	7.9%	12.2%
	W1	35.5%	57.7%
	W2	50.6%	28.5%

References

Bostock, M., Ogievetsky, V., & Heer, J. (2011). D³ Data-Driven Documents. IEEE Transactions on Visualization and Computer Graphics, 17(12), 2301–2309.

Jorgenson, M. T., Y. L. Shur, and E. R. Pullman. 2006. Abrupt increase in permafrost degradation in Arctic Alaska. Geophysical Research Letters 25:L02503.

Kade, A., D. A. Walker, M. K. Raynolds, et al. 2024. Landscape patterns of carbon fluxes in natural and disturbed ice-wedge-polygon tundra. Arctic, Antarctic, and Alpine Research 56:2391244.

Kanevskiy, M., Y. Shur, D. A. (Skip) Walker, et al. 2022. Ice-wedge degradation and stabilization in the Prudhoe Bay Oilfield, Alaska (2011-2022). Page AGU Fall Meeting 2022. Chicago, ILL.

Liljedahl, A. K., J. Boike, R. P. Daanen, et al. 2016. Pan-Arctic ice-wedge degradation in warming permafrost and its influence on tundra hydrology. Nature Geoscience 9:312–318.

Rawlinson, S. E. 1993. Surficial geology and morphology of the Alaskan central Arctic coastal plain. Alaska Division of Geology and Geophysical Surveys, Report of Investigations 93-1.

Raynolds, M. K., D. A. Walker, K. J. Ambrosius, et al. 2014. Cumulative geoecological effects of 62 years of infrastructure and climate change in ice-rich permafrost landscapes, Prudhoe Bay Oilfield, Alaska. Global Change Biology 20:1211–1224.

Walker, D. A., K. R. Everett, P. J. Webber, and J. Brown. 1980. Geobotanical Atlas of the Prudhoe Bay Region, AK, CRREL Report 80-14. Page 69. U.S. Army Cold Regions Research and Engineering laboratory, Hanover, NH.

Walker, D. A. 1985. Vegetation and Environmental Gradients of the Prudhoe Bay Region, Alaska, CRREL Report 85-14. Page 240. CRREL Report 85-14.

Walker, D. A., and K. R. Everett. 1991. Loess ecosystems of northern Alaska: regional gradient and toposequence at Prudhoe Bay. Ecological Monographs 61:437–464.

Walker, D. A., M. K. Raynolds, M. Z. Kanevskiy, et al. 2022. Cumulative impacts of a gravel road and climate change in an ice-wedge-polygon landscape, Prudhoe Bay, Alaska. Arctic Science 8:1040–1056.

Walker, D., A. Breen, et al. 2024. A new ice-rich-permafrost-system observatory on fluvial and lacustrine deposits, Prudhoe Bay Oilfield, Alaska. Pages 752–753 12th International Conference on Permafrost Proceedings Vol. II. Extended abstracts. Whitehorse, Canada.

Witharana, C., M. A. E. Bhuiyan, A. K. Liljedahl, et al. 2021. An Object-Based Approach for Mapping Tundra Ice-Wedge Polygon Troughs from Very High Spatial Resolution Optical Satellite Imagery. Remote Sensing 13:558.